

# A stored energy-based control strategy to improve LVRT capability of HRES using PSO & WCA optimized DVR

DOI : 10.36909/jer.17663

Ashwani Kumar\*, Vishnu Mohan Mishra\*\*, Rakesh Ranjan\*\*\*

\*Research Scholar, Electrical Engineering, Uttarakhand Technical University, Dehradun-248007, India.

\*\*Electrical Engineering, GBPEC, Pauri Garhwal-246194, India.

\*\*\*Vice Chancellor, Himgiri Zee University, Dehradun- 248197, India.

Corresponding Author: [hceashwani@gmail.com](mailto:hceashwani@gmail.com)

## NOMENCLATURE

DFIG	Doubly Fed Induction generator	MW, Mvar	Megawatt, Mega volt ampere reactive
WEC	Wind Energy Conversion	I, $i_{pv}$ , $V_{pv}$	Output current (A) and output voltage (V)
PCC	Point Of Common Coupling	$I_{ph}$	Photocurrent generated by light (A)
LVRT	Low Voltage Ride Through	$R_s$ , $R_{sh}$	Series resistance and shunt resistance ( $\Omega$ )
PSO	Particle Swarm Optimization	n, k	Ideality factor of the cell and the Boltzmann constant ( $1.38 \times 10^{-23} \text{J/K}$ )
ITAE	Integral Time Absolute Error	T	PV cell temperature (K)
FRT	Fault Ride Through	d, q	d-q axis components

## ABSTRACT

The article presented here utilizes the particle swarm optimization (PSO) and water cycle algorithm (WCA) based dynamic voltage restorer (DVR) to augment the low voltage ride through (LVRT) performance of a hybrid renewable energy system (HRES). Moreover, FACT equipment like the dynamic voltage restorer (DVR) is deployed to boost the quick responsiveness of compensation and good transient performance of HRES. Due to numerous disturbances brought on by WECS' nonlinearity, the best tuning of a PI controller for DVR control is investigated to match the LVRT requirement of the HRES. The design incorporates a battery energy storage system (BESS) that is connected over the DC terminals of the DVR to improve the compensating capabilities by regulating the D-Q axis voltage

signal to control the voltage source converter gate signals. In comparison to DVR alone, the suggested technique increases the DC-link voltage and PCC voltage by 44% and 4.6 %, respectively. MATLAB simulation results show that the BESS-enabled PSO DVR performs better in all respect for the compensation of voltage sag and makes the system self-LVRT capable.

**Keywords:** Battery energy storage system; Hybrid renewable energy system; Low voltage ride through; Particle swarm optimization.

## INTRODUCTION

A huge increment in population required high energy demand for the future. In this, renewable energy has significant responsibility to fulfill the electricity demand in a remote areas. For ensuring a stable electrical supply and to reform the size of the resources, hybrid operations of energy are preferred. However, fault issue associated with the HRES has terrible consequences like instability and forces disconnection. The competency of WECS to persist the connection along the short circuit fault raises technical challenges which are labeled as low-voltage ride-through (LVRT) capability. Various solutions, protection schemes, and control strategies were addressed for the LVRT issue in the literature. As in (D. Li & Zhang, 2010) authors proposed a combined protection scheme using a crowbar circuit to protect the RSC during fault intervals. Another study (Jin & Wang, 2010) suggested a hybrid protection strategy to augment the LVRT. Further, a battery energy storage system is coupled to DC bus voltage to mitigate the ripple by applying a DC-link capacitor. (Yang et al., 2016) present the collaborative control strategy between PV converters and static synchronous compensators to improve the LVRT capability of PV systems. The author introduced feed-forward reflection to inject the direct current-link from the PV array to provide grid support. (Yehia, 2014) implemented a super-capacitor energy storage device to mitigate the issue of power fluctuation. The performance of the suggested scheme is analyzed using a voltage profile. Mehta et al. (2015) present the signal stability assessment regarding dynamic performance

DFIG by PSO optimized PI controller. A control strategy is developed consisting of a multilevel STATCOM battery and super-capacitor. Haidar et al. (2015) represent the methodology to enable the system for LVRT without the need for crowbar protection.

The system is studied for different scenarios using real weather data collected. Results show the efficacy of the comprehensive power system control and utility of the proposed HRES. Sahoo et al., (2019) get rid of the issue by using a supercapacitor storage element associated with a series dynamic braking resistor (SDBR), is offered. Super capacitor energy storage (SCES) is equipped along with a DC link which takes care of the power fluctuation. Outcomes declare the impact of the proposed strategy over the traditional control scheme during symmetrical and asymmetrical faults. (Rahim & Nowicki, 2012) suggested an active and reactive control scheme of a super-capacitor energy storage system coordinated along with STATCOM for damping enhancement of the DFIG system. T. Jin et al. (2020) suggest an efficient control strategy for UPQC based on the dq0 detection method to address the drawbacks of current compensation control strategies and boost the compensation effect of UPQC. This work also makes improvements to the space vector pulse width modulation (SVPWM) technique. (Chakraborty et al., 2012) explored the combination of STATCOM and energy storage devices for the operation and control of the HRES. (X. Li et al., 2013) investigate the performance of BESS-based hybrid power systems with battery SOC control. The research was primarily targeted toward control strategies regarding smoothing conditions and capacity. Obando-Montaña et al. (2014) considered STATCOM-based fixed speed generator low voltage ride through enhancement. However, STATCOM needs a crowbar's help to protect the Rotor Side Converter (RSC) of the DFIG from the flow of over-currents. When the voltage is restored, STATCOM decreases the fault clearing time and gives the generator more decelerating torque. The generator's stability margin improves as a result, but the mechanical stress also rises. The utilization of a DVR is a suitable choice since it operates without the need for another safety circuit. Jayaprakash et al. (2014) proposed a

control technique having a capacitor embedded which reduced the rating DVR. Hassanein et al., (2020) article proposed an artificial neural network (ANN) technique for DVR to boost the response of an isolated HRES. ANN is employed for optimization of PI controllers with application of managing the load profile. Also DVR-VSI coordinated the pulses at distinct anomalous running conditions, and transforms the PI controller into robust one appropriately. The scheme execution with the recommended ANN-DVR controller is done by building up the electrical characteristics. The system performance in addition to the recommended ANN-DVR controller is found improved. By employing the compensation strategy of faulty power lines, the whole power network remains standing stable. Engagement of the HRES at the time of fault incident and therefore raise the LVRT capability. The significant novel addition of this article is using BESS enabled PSO and WCA controlled DVR to strengthen the HRES against LVRT. A comparison among different techniques for regulating LVRT control strategies is summarized. The majority of the research that has been published so far has concentrated on LVRT augmentation of single renewable energy grid-connected power plants. Since large-scale hybrid energy power plants have not yet been tried for LVRT upgrading. This study's primary contribution is its suggestion that an energy storage-based DVR should be installed to support the LVRT functionality of HRES. The research also suggests an efficient control structure that gives HRES the capacity to use LVRT to adhere to grid code requirements. PSO & WCA-based DVR and BESS are used in the structure to give the system the ability to supply the active and reactive power needed when the voltage drops. The HRES with a 9.0 MW DFIG-based variable speed WT and a 1 MW capacity PV plant has been taken into consideration for testing. In comparison to other strategies that have been reported, simulation results demonstrated that the proposed strategy performed better.

#### **SYSTEM DESCRIPTION MODEL OF PV ENERGY SOURCE**

The structure of a PV plant integrated with a power grid may have many types of

architecture (Naceur et al., 2021). Here PV plant with a DFIG-based wind plant is integrated with the grid. The PV plant module consists of 5 series with 660 parallel strings.

For the PV model representation, a single diode equivalent circuit is shown in Fig.1 (a)

$$I_L = I_{ph} - I_D - I_{sh} = I_{ph} - I_o \left[ \exp\left(\frac{V_{pv} + I_L R_s}{a}\right) - 1 \right] - \frac{V_{pv} + I_L R_s}{R_{sh}} \quad (1)$$

$$a = \frac{nkT}{q} \quad (2)$$

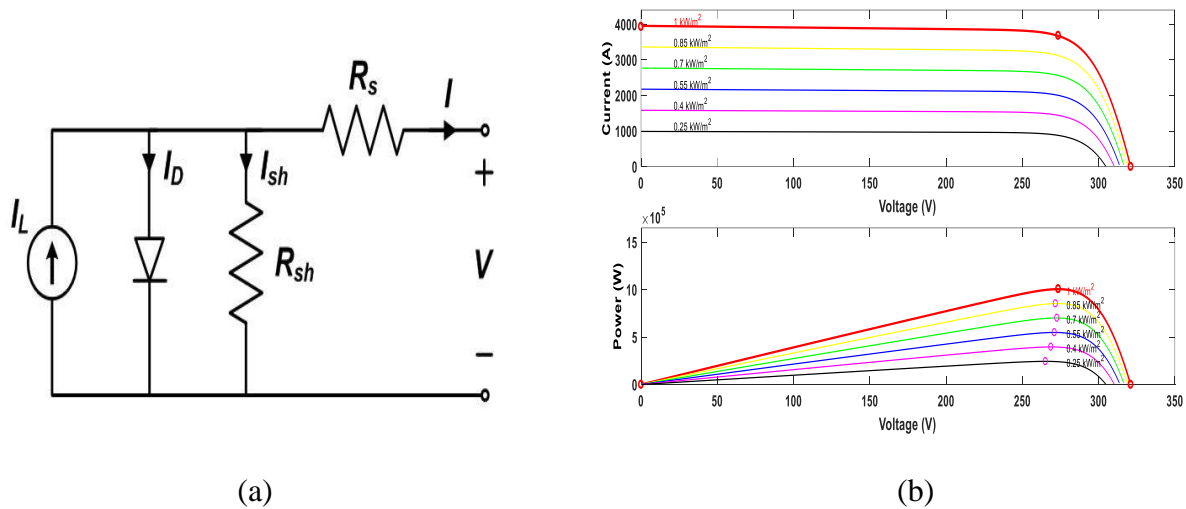


**Figure 1.** (a) Single diode equivalent circuit of PV model (b) Effect of variation in solar irradiance on I-V and P-V characteristics of modules.

Where  $I_L$ ,  $I_o$ ,  $R_s$ ,  $R_{sh}$ ,  $a$  and  $V_T$  represents the photocurrent (A), the saturation current of a diode (A), series resistance ( $\Omega$ ), shunt resistance ( $\Omega$ ), ideality factor of a diode, and the equivalent value of thermal voltage (V) respectively. Fig.1 (b) shows the current and power variation concerning voltage for the PV module at the different levels of solar irradiance. (Iqbal M et al., 2022) The different MPPT control method scheme in literature perturb and observe is adopted here.

### MODELLING OF DFIG WIND TURBINE AND DVR

WT is used to capture the kinetic energy from the wind and convert it into mechanical power.

The wind plant consists of six WT of 1.5MW capacity. The main parts of DFIG are a wound rotor induction generator, and a bidirectional voltage converter with DC-link (Mohamed et al., 2020). The stator part of DFIG is linked to the grid synchronized with the required frequency on the other hand rotor is fed through an electronic converter as shown in Fig.2.

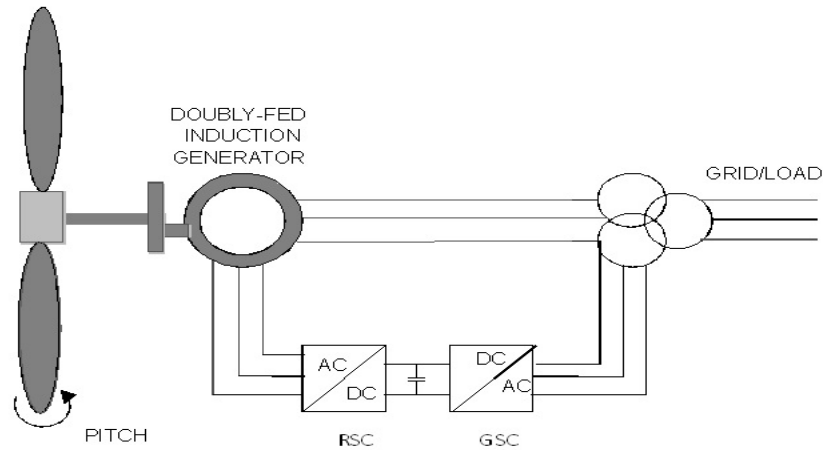


**Figure 2.** Mathematical modeling of DFIG-based WT

The synchronously rotating frame may be used to represent the vector model of DFIG. The voltage equation in the d-q park model is used to write the dynamic model.

### CONTROL STRATEGY AND MODELLING OF DVR

DVR is bespoke power equipment that inserts sufficient voltage into the structure to optimize the non-linear load's voltage profile. The essential components of a DVR are a DC supply, a power electronic IGBT converter, and a transformer in series with a connected load. To compensate for the voltage sag, it injects the appropriate compensating voltage. The rating of DVR is selected by the in-phase compensation method. The voltage inserted by the DVR may be dictated as:

$$V_{DVR} = V_L + Z_{TH} I_L - V_{TH} \quad (3)$$

$$I_L = \frac{P_L + jQ_L}{V} \quad (4)$$

Here  $V_L$ ,  $Z_{TH}$ ,  $I_L$ , and  $V_{TH}$  represent the load voltage load impedance load current, and system voltage respectively. The load current  $I_L$  is depicted as

Here  $V_L$  is considered a reference

$$V_{DVR}^* = V_L^{\angle 0} + Z_{TH}^{\angle(\beta-\theta)} - V_{TH}^{\angle\delta} \quad (5)$$

$$\text{With } \theta = \tan^{-1}\left(\frac{\theta_L}{P_L}\right) \quad (6)$$

The power output of DVR in complex form can be depicted as

$$S_{DVR} = V_{DVR} I_{DVR}^* \quad (7)$$

The in-phase compensated rated power of DVR may be written as:

$$S_{DVR} = \sum_{k=a,b,c} V_{DVR,k}^{ref} * I_L \quad (8)$$

$$P_{DVR} = P_L - P_g \quad (9)$$

Here  $V_{DVR,k}^{ref}$  is the root mean square value of injected DVR voltage in phase k and  $I_L$  is the RMS of load current. The active power feed by DVR is

$$P_{DVR} = (3 * V_L * I_L * \cos\theta) - \sum_{k=a,b,c} [V_{DVR,k}^{ref} * I_L * \cos\psi] \quad (10)$$

$$V_{DVR,k}^{ref} = \sqrt{2} * |V_L - V_{g,k}^{ref}| \text{ and } k = a, b, c \quad (11)$$

The phase angle of injected voltage should be the same as utility voltage. The DVR in the synchronous reference frame is controlled by the required magnitude of the load bus voltage respectively

$$V_{La}^* = V_0 \sin \omega t \quad (12)$$

$$V_{Lb}^* = V_0 \sin \left( \omega t - \frac{2\pi}{3} \right) \quad (13)$$

$$V_{Lc}^* = V_0 \sin \left( \omega t + \frac{2\pi}{3} \right) \quad (14)$$

The basic control structure relies on supply voltage and phases angle to derive the level of compensating voltage.

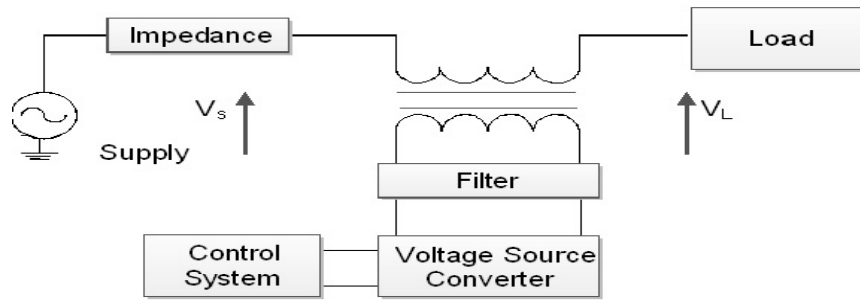


**Figure 3.** DVR configuration with supply system and load.

The working of the synchronous dq-reference frame allows easy clamping of injection voltage. It enables DVR to mitigate the sag and maintain a sinusoidal voltage profile. The operation of control is synchronized with input voltage by PLL. The control generates the dq reference which is transformed to three-phase stationary values for the generation of the PWM modulation signal. Further, the compensating voltage is fed by the transformer to the utility at PCC as depicted in Fig.3.

### BATTERY ENERGY STORAGE SYSTEM

A battery energy storage system (BESS) which is a storage device is combined across the DC-Link capacitor. The purpose is to connect the BESS to adjust the voltage, which maintains the DC capacitor voltage. In the case of voltage sag, it supplies the reactive power to achieve a stable system rapidly. BESS is integrated with the DC capacitor of DVR to exchange the active and reactive power in-between DVR and HRES. P & Q power exchange expressed by

$$P = \frac{V_{pcc} V_c \sin(\alpha)}{X} \quad (15)$$

$$Q = \frac{V_{pcc} (V_{pcc} - V_c \cos(\alpha))}{X} \quad (16)$$

Where  $V_c$ ,  $P$ , and  $Q$  depicts the inverter voltage, active power exchange, and reactive power exchange respectively. Also,  $V_{pcc}$ ,  $\alpha$ , and  $X$  are the voltage at the PCC, angle concerning  $V_c$ , and reactance of the coupling inductor.

### PARTICLE SWARM OPTIMIZATION

PSO is a stochastic optimization technique based on a computer population. The solution of a

swarm of particles is included in this algorithm, and these particles move in their search space as shown in Fig. 4.

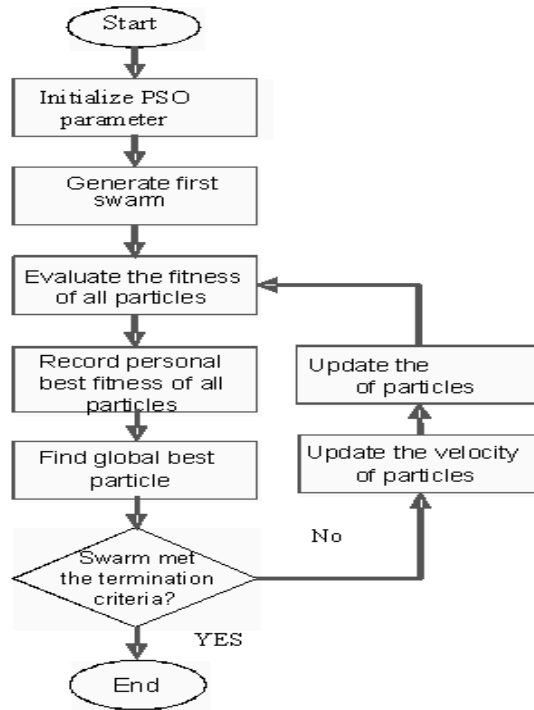


**Figure 4.** Flowchart of the PSO

The concept behind this optimization method is based on the behavior of some biological animals. The velocity of each new dimension in the next iteration, and that updated velocity is utilized to find the particle's new position. (Eltamaly et al., 2021). In this method, the particle's state is continuously updated in the multi-dimensional search space until the particle reaches its ideal state. (Kumar et al., 2022) Various vectors are described as follows to mathematically define the PSO technique:

Assume there are  $N$  particles involved in the process. The position vector  $X_i = (X_{i1}, X_{i2}, \dots, X_{id}, \dots, X_{iD})$  is moved in  $D$ -dimensional space for each particle.

Their velocity vector may be defined as  $V_i = (V_{i1}, V_{i2}, \dots, V_{id}, \dots, V_{iD})$  and their position vectors  $P_i = (P_{i1}, P_{i2}, \dots, P_{id}, \dots, P_{iD})$ . The swarm's optimal position vector is denoted as  $P_g = (P_{g1}, P_{g2}, \dots, P_{gd}, \dots, P_{gD})$  then the update formula of the individual's optimal position is

$$p_{i,t+1}^d = \begin{cases} x_{i,t+1}^d, & \text{if } f(X_{i,t+1}) < f(P_{i,t}) \\ p_{i,t}^d, & \text{otherwise} \end{cases} \quad (17)$$

The updated velocity and position formula for the swarm's ideal position is as follows:

$$v_{i,t+1}^d = v_{i,t}^d + c_1 * rand * (p_{i,t}^d - x_{i,t}^d) + c_2 * rand * (p_{g,t}^d - x_{i,t}^d) \quad (18)$$

$$x_{i,t+1}^d = x_{i,t}^d + v_{i,t+1}^d \quad (19)$$

## SIMULATION RESULTS AND PERFORMANCE EVALUATION

The suggested FRT technique is simulated using a MATLAB environment. DFIG considered here has 1.5 MW, a total of 9 MW wind turbines these turbines are supplied with 15 m/sec. with this a PV system is also integrated with 1 MW capacity. The introduced system is tested with PSO and WCA optimized PI controller to mitigate the sag. A battery energy system is also integrated to improve the FRT capability. For this, a three-phase symmetrical 3-phase to ground fault is created at the PCC which is initiated at 0.4s and withdrawn at 0.6s. Three different types of control schemes are compared to confirm the effectiveness of the suggested scheme. In this section, DVR is implemented at the PCC of HRES. The PI controller of DVR is optimized by PSO and WCA to set the LVRT requirement according to the grid code. Here the analysis of the DC link voltage of DFIG is done in Fig.5 where it is observed that in case when DVR is not employed the DC link voltage value rises up to 2192 volts during the 0.4s to 0.6s. After the support of WCA algorithm-based DVR rise in DC voltage gets reduced and varies up to 876 volts and gets stabilized than previous. Further incorporation of PSO tuned DVR could enable to atone for the bigger fluctuation in an improved way. It is recognized that

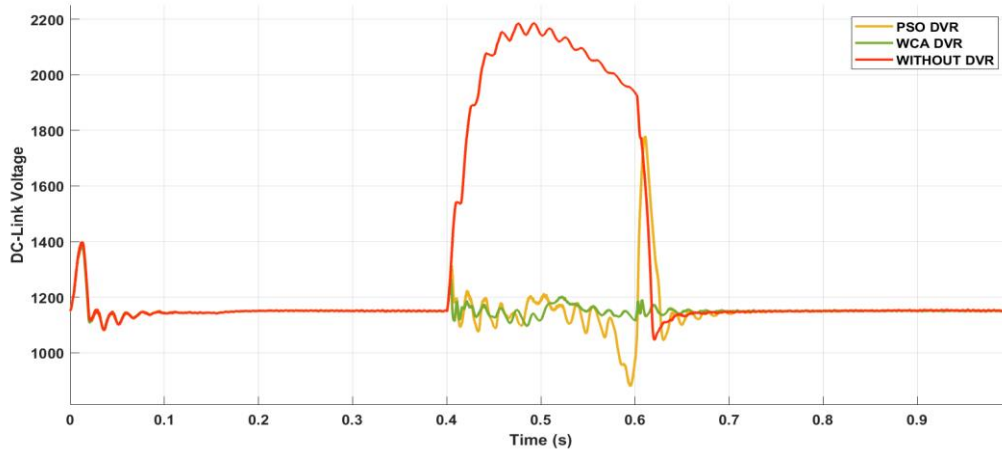


**Figure 5.** Performance of HRES DC-link voltage.

PSO tuned device is capable to maintain the voltage across DC-link voltage within 1210 volts. This controlling technique is realized best of all. The below Fig.6 depicts the voltage at PCC with a different type of control strategy. When no DVR is connected to the system  $V_{pcc}$  does not comply with the grid code.

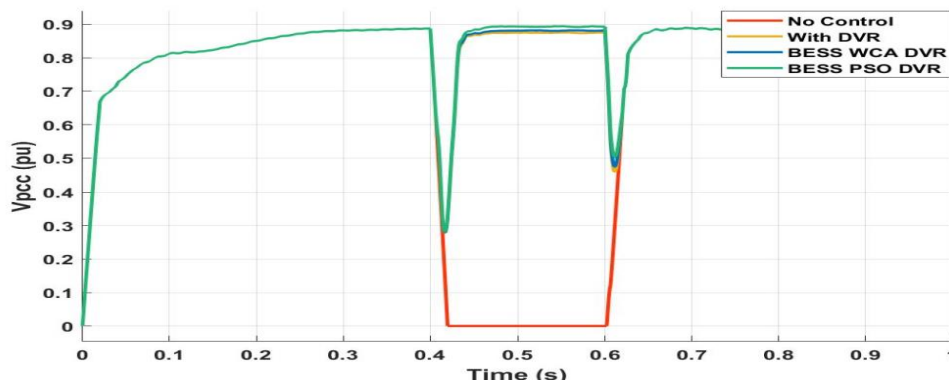


**Figure 6.** Performance of HRES voltage at PCC (pu).

Thereafter DVR is introduced in the system by which  $V_{pcc}$  reaches 0.87 pu. Also, the BESS-based DVR is connected and WCA optimized PI carries the  $V_{pcc}$  to the 0.89pu during 0.4s-0.6s. Much improvement can be observed when we employ BESS based PSO tuned PI controller. This leads  $V_{pcc}$  to the 0.9pu, giving better performance. LVRT performance is improved by the BESS connected to the DC-link terminal to improve the voltage sag performance. Fig. 7. shows the voltage, current, SOC, and power response of the energy storage system.

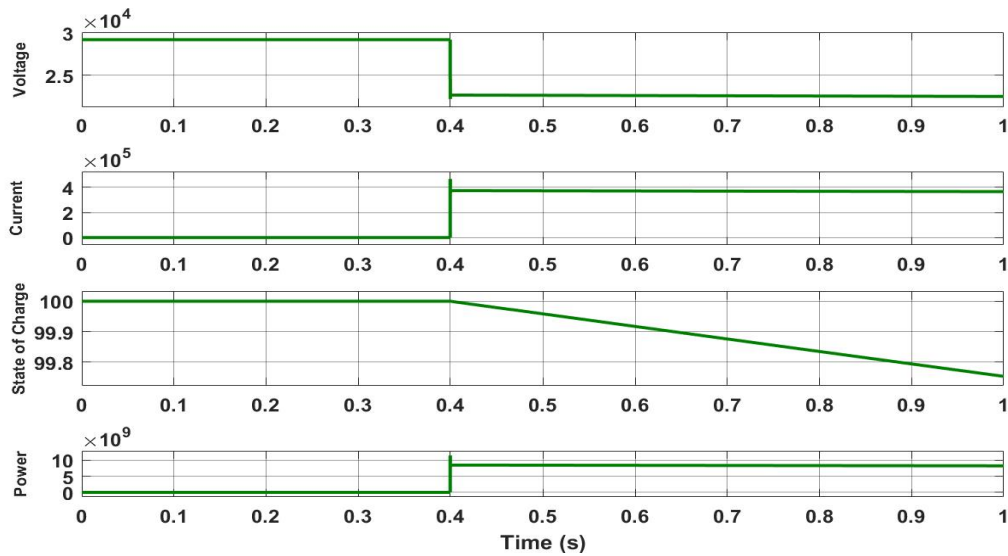


**Figure 7.** Performance of battery energy storage system.

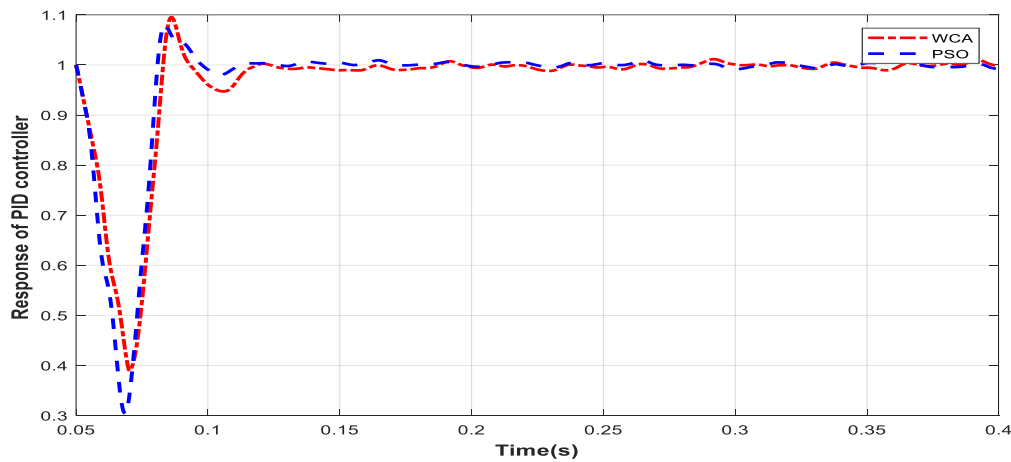


**Figure 8.** Performance PID controller based upon PSO and WCA.

On the occurrence of fault voltage, the battery get discharged and starts feeding current to the fault zone. The third part of Fig.7 depicts that SOC levels start decreasing after 0.4s. Also power graph from energy storage clearly shows the power support to the PCC during the voltage sag. Fig. 8. shows the comparison of the PID response between PSO and WCA algorithm. It is the observer that the PSO performs better than WCA to control the PID controller. DVR measures the system reference voltage (pu) and compares it with a reference value, the return error is fed to a PI controller to produce the angle  $\alpha$ , called the firing angle. To control the DVR, d and q-axis reference values are derived from PI controllers. PSO and

WCA algorithm is implemented to identify the optimal gain of PI controller of the DVR. Integral time absolute error (ITAE), is used as performance indices for control. It is expressed in equation (20) in which error is generated by taking the set point value and system actual output of the system.

$$ITAE = \int_0^{\infty} t(|V_{dc_{ref}} - V_{dc}|) dt \quad (20)$$

Where  $V_{dc_{ref}}$  is the reference DC voltage in volts,  $V_{dc}$  actual DC voltage of DC voltage controller and run time for simulation is  $t$ . The value of ITAE obtained with PSO and WCA is 0.0045 and 0.0048 respectively.

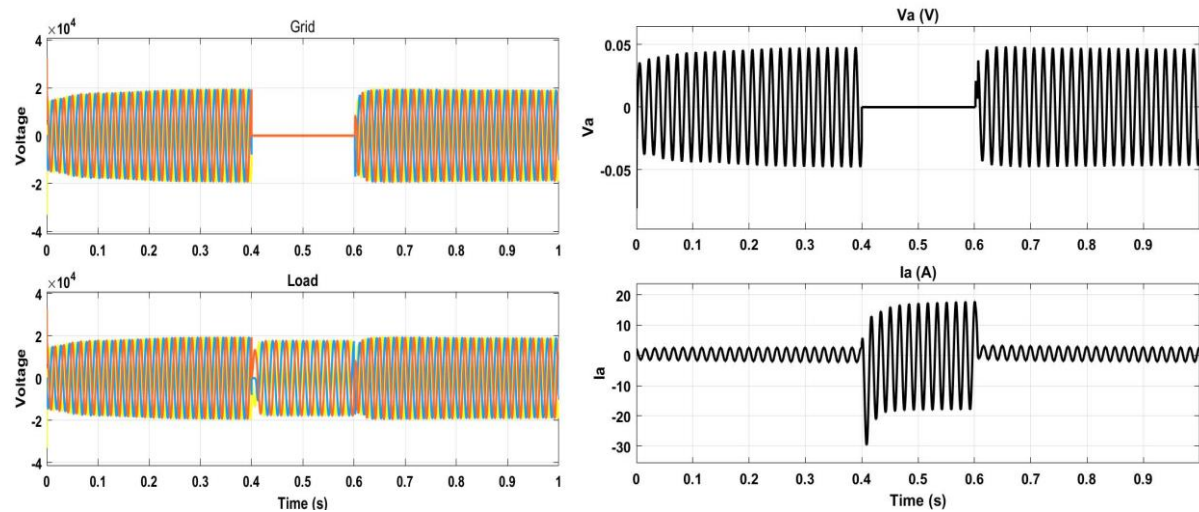


**Figure 9.**(a) The voltage at PCC without and with PSO compensation. (b) Voltage and current profile across PV plant (pu).

Fig. 9 (a) Shows the voltage profile at the PCC in both the cases i.e. load voltage and injected voltage waveform during three-phase voltage sag. When DVR is not employed and when the PSO tuned PI controller based DVR compensates for the fault. Fig.9 (b). depicts the voltage and current of the PV plant subjected to the three-phase fault. Also wind speed of the DFIG is shown in Fig. 10, where the fault initiates at 0.4s and continues till 0.6s.

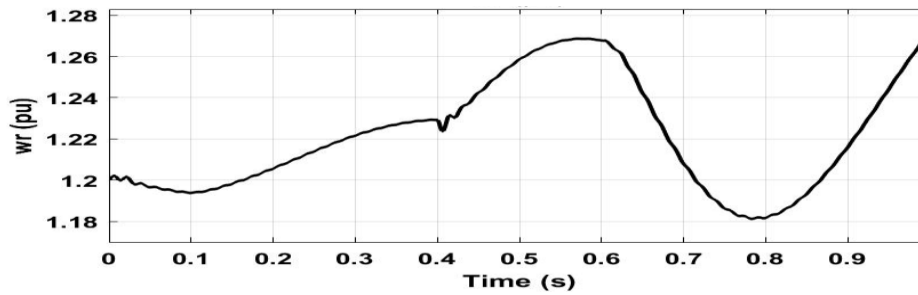


**Figure 10.** Wind speed curve of DFIG subjected to  $3\Phi$  fault.

The simulation results depict that the PSO optimized PID controller for energy storage embedded with DVR shows better results as compared to WCA-based DVR in terms of performance indices ITAE as shown in table 1.

Table 1. Comparison of ITAE with WCA and PSO algorithm.

Performance Indices	Algorithm	Controller	Value	Iteration
ITAE	WCA	PID	0.0048	100
ITAE	PSO	PID	0.0041	100

## CONCLUSION

This paper explored the outcome of BESS enabled, PSO, and WCA tuned DVR on the LVRT capability improvement in HRES consisting of DFIG-based wind plants with PV plants. The DVR performance is improved by introducing a BESS to the DC-link of the DVR. Also in this approach PI controller is tuned by PSO and WCA algorithm. This manages the decrease in voltage sag improved in PSO configuration as compared to WCA during fault time. Further, the addition of BESS to the DC-link makes HRES capable to provide active power into the grid during and post fault conditions. Along with this configuration, improved control of sag mitigation becomes possible. From the above analysis, it is confirmed that DVR can effectively mitigate the LVRT issues in HRES. The verification of the recommended control approach and outcome on HRES is implemented using simulation in MATLAB.

## REFERENCES

Chakraborty, A., Musunuri, S. K., Srivastava, A. K., & Kondabathini, A. K. (2012).

- Integrating STATCOM and battery energy storage system for power system transient stability: A review and application. *Advances in Power Electronics*, 2012.  
<https://doi.org/10.1155/2012/676010>
- Eltamaly, A. M., Abdelaziz, A. Y., & Abo-Khalil, A. G. (2021). *Control and Operation of Grid-Connected Wind Energy Systems*.  
<https://books.google.com/books?hl=en&lr=&id=gqkhEAAAQBAJ&oi=fnd&pg=PR5&dq=technology+of+wind+energy&ots=FykAhG-w4D&sig=SHJhmVx0Aj2rqE5ueMUW2syPHgY%0Ahttp://link.springer.com/10.1007/978-3-030-64336-2>
- Haidar, A. M. A., Hagh, M. T., & Muttaqi, K. M. (2015). Improving low voltage ride-through using super capacitor at the DC link of Doubly-Fed Induction Generator based wind turbine. *Proceedings of the Universities Power Engineering Conference, 2015-Novem*, 1–6. <https://doi.org/10.1109/UPEC.2015.7339855>
- Hassanein, W. S., Ahmed, M. M., Osama abed el-Raouf, M., Ashmawy, M. G., & Mosaad, M. I. (2020). Performance improvement of off-grid hybrid renewable energy system using dynamic voltage restorer. *Alexandria Engineering Journal*, 59(3), 1567–1581.  
<https://doi.org/10.1016/j.aej.2020.03.037>
- Iqbal M, M., Badar, A., C.V, P., K, N., & Yousuff, M. (2022). Fuzzy gain Scheduled PID Controller for Power Quality Enhancement in Grid Connected Hybrid Solar PV-PEMFC Energy *Journal of Engineering Research*, 1–16. <https://doi.org/10.36909/jer.15593>
- Jayaprakash, P., Singh, B., Kothari, D. P., Chandra, A., & Al-Haddad, K. (2014). Control of reduced-rating dynamic voltage restorer with a battery energy storage system. *IEEE Transactions on Industry Applications*, 50(2), 1295–1303.  
<https://doi.org/10.1109/TIA.2013.2272669>
- Jin, C., & Wang, P. (2010). Enhancement of low voltage ride-through capability for wind turbine driven DFIG with active crowbar and battery energy storage system. *IEEE PES General Meeting, PES 2010*. <https://doi.org/10.1109/PES.2010.5588180>
- Kumar, D. G., Ganesh, A., & Bhoopal, N. (2022). THD optimization in 15-level asymmetric reduced switch count multilevel PV inverter using optimization algorithms. *Journal of Engineering Research*, 1–16. <https://doi.org/10.36909/jer.13673>
- Li, D., & Zhang, H. (2010). A combined protection and control strategy to enhance the LVRT capability of a wind turbine driven by DFIG. *2nd International Symposium on Power Electronics for Distributed Generation Systems, PEDG 2010*, 50807035, 703–707.  
<https://doi.org/10.1109/PEDG.2010.5545850>

- Li, X., Hui, D., & Lai, X. (2013). Battery energy storage station (BESS)-based smoothing control of photovoltaic (PV) and wind power generation fluctuations. *IEEE Transactions on Sustainable Energy*, 4(2), 464–473. <https://doi.org/10.1109/TSTE.2013.2247428>
- Mehta, B., Bhatt, P., & Pandya, V. (2015). Small signal stability enhancement of DFIG based wind power system using optimized controllers parameters. *International Journal of Electrical Power and Energy Systems*, 70, 70–82. <https://doi.org/10.1016/j.ijepes.2015.01.039>
- Mohamed, M. A., Diab, A. A. Z., Rezk, H., & Jin, T. (2020). A novel adaptive model predictive controller for load frequency control of power systems integrated with DFIG wind turbines. *Neural Computing and Applications*, 32(11), 7171–7181. <https://doi.org/10.1007/s00521-019-04205-w>
- Naceur, F. Ben, Saidi, A. S., Bhutto, J. K., & Mahjoub, M. A. (2021). An Advanced MPPT Scheme for Standalone Solar powered System using Neuro-Fuzzy based on measured data. *Journal of Engineering Research*, 1–15. <https://doi.org/10.36909/jer.12535>
- Obando-Montaña, A. F., Carrillo, C., Cidrás, J., & Díaz-Dorado, E. (2014). A STATCOM with supercapacitors for low-voltage ride-through in fixed-speed wind turbines. *Energies*, 7(9), 5922–5952. <https://doi.org/10.3390/en7095922>
- Rahim, A. H. M. A., & Nowicki, E. P. (2012). Supercapacitor energy storage system for fault ride-through of a DFIG wind generation system. *Energy Conversion and Management*, 59, 96–102. <https://doi.org/10.1016/j.enconman.2012.03.003>
- Sahoo, S. S., Chatterjee, K., & Tripathi, P. M. (2019). A coordinated control strategy using supercapacitor energy storage and series dynamic resistor for enhancement of fault ride-through of doubly fed induction generator. *International Journal of Green Energy*, 16(8), 615–626. <https://doi.org/10.1080/15435075.2019.1602531>
- Yang, L., Liu, W., Peng, G., Chen, Y. G., & Xu, Z. (2016). Coordinated-Control Strategy of Photovoltaic Converters and Static Synchronous Compensators for Power System Fault Ride-Through. *Electric Power Components and Systems*, 44(15), 1683–1692. <https://doi.org/10.1080/15325008.2016.1194502>
- Yehia, D. M. (2014). *DFIG-Based Wind Turbine with Supercapacitor Energy Storage*. 187–190.